International Journal of Environmental Sciences
ISSN: 2229-7359
Vol. 11 No. 22s, 2025
https://theaspd.com/index.php

Magnetic and Electric Properties of Pbtio$_3$- $Y_3Fe_5O_{12}$ Ceramic Composites

T. Susneha[1], K. Samba Siva Rao[2], N.V. Prasad[1]
[1]Materials Research Laboratory, Department of Physics, Osmania University, Hyderabad 500007, India.
[2]Advanced Magnetics Group, Defence Metallurgical Research Laboratory, Hyderabad 500 058, India
*Author for correspondence: nvp1969@rediffmail.com

Abstract:
The aim of the work is to fabricate the (1-x) $PbTiO_3$ (PT) - x $Y_3Fe_5O_{12}$ (YIG), where x takes values of 20, 30, 65, and 80, using the standard solid-state sintering method, with ball milling employed to mix the components before sintering at 1000°C. The structural and magnetic properties of the composites were then evaluated. The results demonstrate PT and YIG phases coexist without any secondary phase. The observed Raman active mode confirms the presence of cubic and tetragonal phases of YIG and PT. SEM photographs have shown both larger spherical and small shape grains. The magnetic and electrical characteristics are determined by the ferroelectric and magnetic hysteresis loops. The composite exhibits a maximum saturation magnetization of approximately 27 emu/g for higher YIG and lower PT (80 YIG-20PT) content among all the composites. PT is well-known toxic material; however, one cannot replace this material to another lead-free material. To achieve environment-friendly, non-lead material such as YIG-based PT composites are being prepared. Based on the law of approach to saturation (LAS) and ferroelectric hysterics loops, it is concluded that the strong magnetic and electric coupling interaction for 80YIG-20PT acts as a key role and helpful to fabricate the multi-dielectric or magnetodielectric device.
Key words: *YIG-PT composite, Raman modes, LAS, electric and magnetic ferroelectric hysteresis loops.*

INTRODUCTION

The modified garnets family is being received interest owing to the fact of its inherent insulating strong magnetic properties at RT. The structure of YIG is cubic system with space group Ia3d containing 8-formula units per unit cell. Yttrium ions occupy dodecahedral (24c) sites. Iron ions are distributed over tetrahedral (24d) sites and octahedral (16a) sites. On account of its unique magnetic properties, many researchers are concentrating both electrical and magnetic properties on modified YIG ceramics. In our earlier results and based on the reports, it is revealed that the non-magnetic ion modified YIG has shown improved magnetic properties [1-4].

Yttrium Iron Garnet (YIG) - barium ttitanate ($BaTiO_3$) composites have shown distinctive multiferroic properties and therefore they found attractive candidates for technological innovations[5]. YIG is known for its excellent magnetic characteristics, including low magnetic loss, high permeability, and strong performance in microwave-antenna applications[1]. These unique attributes have led to its widespread use in functional devices [1-3]. YIG is also utilized for energy harvesting, magnetic, and electromagnetic shielding applications[5]. However, few research reports is being available on Yttrium Iron Garnet (YIG)-based composites. Recent reports on piezo-magnetic of similar composites have shown remarkable exchange coupling properties[5]. These composites are of great interest because the combine magnetic and piezoelectric or ferroelectric characteristics of these materials. This makes them highly promising for applications in magnetoelectric devices, spintronics, and other multifunctional systems [5-15].

On the other hand, $PbTiO_3$ (PT), a ferroelectric ceramic, is renowned for its outstanding piezoelectric and ferroelectric behaviour. These materials have shown applications in electronic devices such as piezoelectric sensors, actuators, capacitors, etc. [16,17]. $PbTiO_3$ also plays a crucial role in energy harvesting applications, where it efficiently converts mechanical stress into electrical energy [17]. $PbTiO_3$ has also shown remarkable displacive - ferroelectric transitions as the inelastic scattering of soft optic phonons of $PbTiO_3$ prompted many researchers in the optoelectronic field. While YIG and $PbTiO_3$ materials are utilized extensively in various applications, but the potential for combining these materials in composite form has garnered limited attention. The integration of YIG, with its magnetic properties, and $PbTiO_3$, with its piezoelectric and ferroelectric properties, could lead to the creation of magnetoelectric composites, where the coupling of magnetic and electric responses could open up new possibilities. Despite this potential, there is a noticeable lack of research that focuses on the synthesis and application of YIG-$PbTiO_3$ ceramic composites.

In pprevious work, we synthesized YIG materials via solid-state reactions [18]. Building on this foundation, the present study investigates the development of YIG-$PbTiO_3$ particulate composites through solid-state synthesis. The goal is to assess how varying the ratio of $PbTiO_3$ affects the magnetic and other functional properties of these composite materials. Specifically, we explore compositions of YIG and $PbTiO_3$ with varying weight percentages, x YIG - (1-x) PT, where x takes values of 20, 30, 65, and 80. A detailed electrical, magnetic and Raman studies were reported in this work.

METHODOLOGY

In this study, Yttrium Iron Garnet (YIG) was chosen as the magneto strictive phase, while lead titanate ($PbTiO_3$) was selected as the ferroelectric phase. YIG was synthesized using a solid-state synthesis approach, with Y_2O_3 (Sigma Aldrich) and Fe_2O_3 (Sigma Aldrich) serving as the starting materials. The required stoichiometric amounts of the powders were carefully combined and subjected to ball milling in the presence of ethanol as a grinding medium. Following this, the wet mixture was dried, and the dried sample was ground once again for 30 minutes. The resulting powder underwent calcination first at 1200°C, and then at 1250°C for 4 hours, with intermediate grinding to ensure uniformity throughout the process. Similarly, $PbTiO_3$ was synthesized through a solid-state synthesis method. The reactant materials were g PbO and TiO_2. The materials were mixed in the exact stoichiometric ratio required for the formation of $PbTiO_3$. The first step in the process involved thorough grinding of the powder mixture using a planetary ball mill for a duration of 24 hours with 150 rpm. During this grinding process, ethanol was used as the grinding medium to prevent particle agglomeration. After the grinding process, the wet powder was dried overnight under an infrared lamp to remove any residual ethanol and moisture. Once dried, the powder was sieved through a 200-mesh sieve and further ground for an additional hour using an Agate mortar and pestle. The powder was then formed into pellets using a hydraulic-press, with polyvinyl alcohol (PVA) used as a binder. To prevent the evaporation of lead during the heating process, the green pellets were carefully placed in a bed of lead oxide [19, 20]. This step is crucial, as lead has a high vapor pressure at elevated temperatures, and its loss would alter the stoichiometry and affect the final properties of the material. By surrounding the pellets with lead oxide, it ensures that any lead vaporized during calcination can recombine with the oxide, thus maintaining the necessary lead content in the material. The pellets were then subjected to a two-step calcination process. The first calcination step took place at 800°C, which allows for initial phase development and solid-state reactions between the lead oxide and titanium oxide. The second calcination step, conducted at 900°C for 4 hours, ensures the complete crystallization of the desired $PbTiO_3$ phase.

For the preparation of the multiferroic composite, Yttrium Iron Garnet (YIG) and Lead Titanate (PT) were combined in specific weight ratios, following the formula (x) wt% YIG - (1-x) wt% $PbTiO_3$, where x was set to values of 20, 30, 65, and 80. The powders of both materials were thoroughly blended using an Agate mortar and pestle to ensure an even mixture. After blending, the powder was compacted into 10 mm diameter pellets. These pellets were then subjected to a sintering process in a furnace at 1000°C for a duration of 4 hours to facilitate the solid-state formation of the composite.

To analyse the phase and structure of the synthesized materials, X-ray diffraction (XRD) measurements were conducted with an Xpert Panalytical diffractometer, utilizing Cu K_α radiation (λ=1.54056 Å). Scanning electron microscope (SEM) pictures were taken on the fine polished YIG-PT composites with the help of microscope model ZEISS FESEM.

Vibrational properties of the composite were assessed at ambient temperature through Raman spectroscopy, employing a 785 nm laser from a Horiba Jobin Yvon system. The ferroelectric behaviour was examined by recording the polarization-electric field (P-E) hysteresis loops at room temperature, using pellets with a silver electrode as the test samples. For evaluating the magnetic characteristics, a vibrating sample magnetometer (Lake Shore) was used to determine the magnetic response of the composites under an external magnetic field up to 5000 Oe.

RESULTS AND DISCUSSION

Figure 1 illustrates the XRD patterns of YIG/PT composites with varying weight percentages. The results clearly indicate that both YIG and PT phases are present in the composites. As the percentage of YIG increases, a decrease in the intensity of the (4 2 0) peak is observed (marked as # in the Fig 1). All the Bragg diffraction peaks corresponding to YIG and PT match well with the JCPDS reference files #555980

and #1102397, respectively. The characteristics of these peaks, including their intensity and position, vary with the composite's composition. Table 1 provides the 2θ and intensity values for the primary peaks at (1 0 1) and (4 2 0). As increasing the YIG content, the intensity of (1 0 1) peak of PT decreases and finally disappears. On the other hand (4 0 0) peak of YIG shows the same trend. This is considered to be the hetaeristic nature of the present composites. This change could be attributed to variations in internal strain resulting from the interaction between the ferroelectric and ferromagnetic lattices in the composite. Similar observations were reported by Avanish et al. [20].

Figure 1. XRD patterns of YIG,PT and its composites.

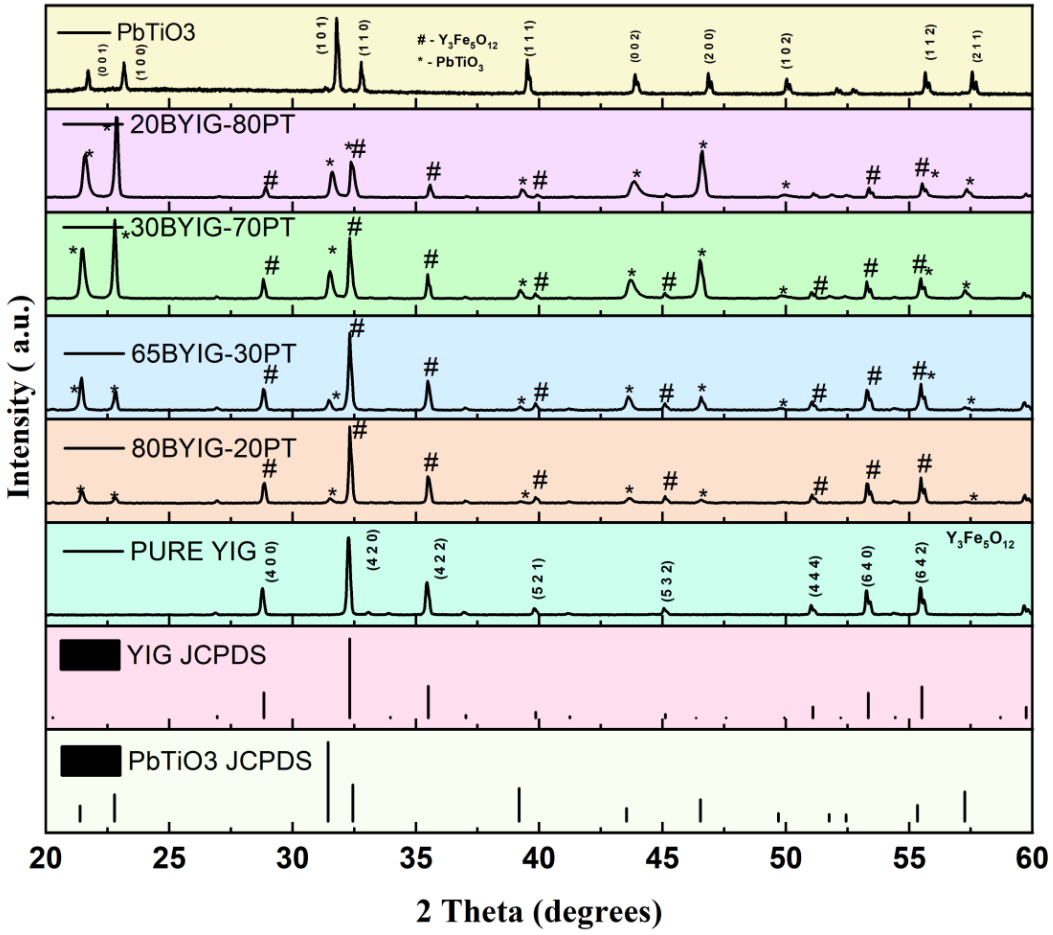

SNo.	Sample Name	Sample Code	2Theta at (1 0 1)	Intensity at (1 0 1)	2Theta at (4 2 0)	Intensity at (4 2 0)
1	Pure PT (PbTiO3)	PT	31.780	44933	-	-
2	20YIG-80PT	YP2	31.618	12597	32.370	17007
3	30YIG-70PT	YP3	31.518	11103	32.320	22166
4	65YIG-35PT	YP6	31.468	6247	32.320	28139
5	80YIG-20PT	YP8	31.518	5067	32.320	33465
6	Pure YIG (Y3Fe5O12)	YIG	-	-	32.270	42317

Table 1. XRD Intensities of Bragg peaks of YIG-PT composites

International Journal of Environmental Sciences
ISSN: 2229-7359
Vol. 11 No. 22s, 2025
https://theaspd.com/index.php

Fig 2(a-d) show SEM micrographs of the PT-YIG composite ceramics. The grain size was calculated, using image-J software. The average grain size was found to increase with increasing the YIG composition (see

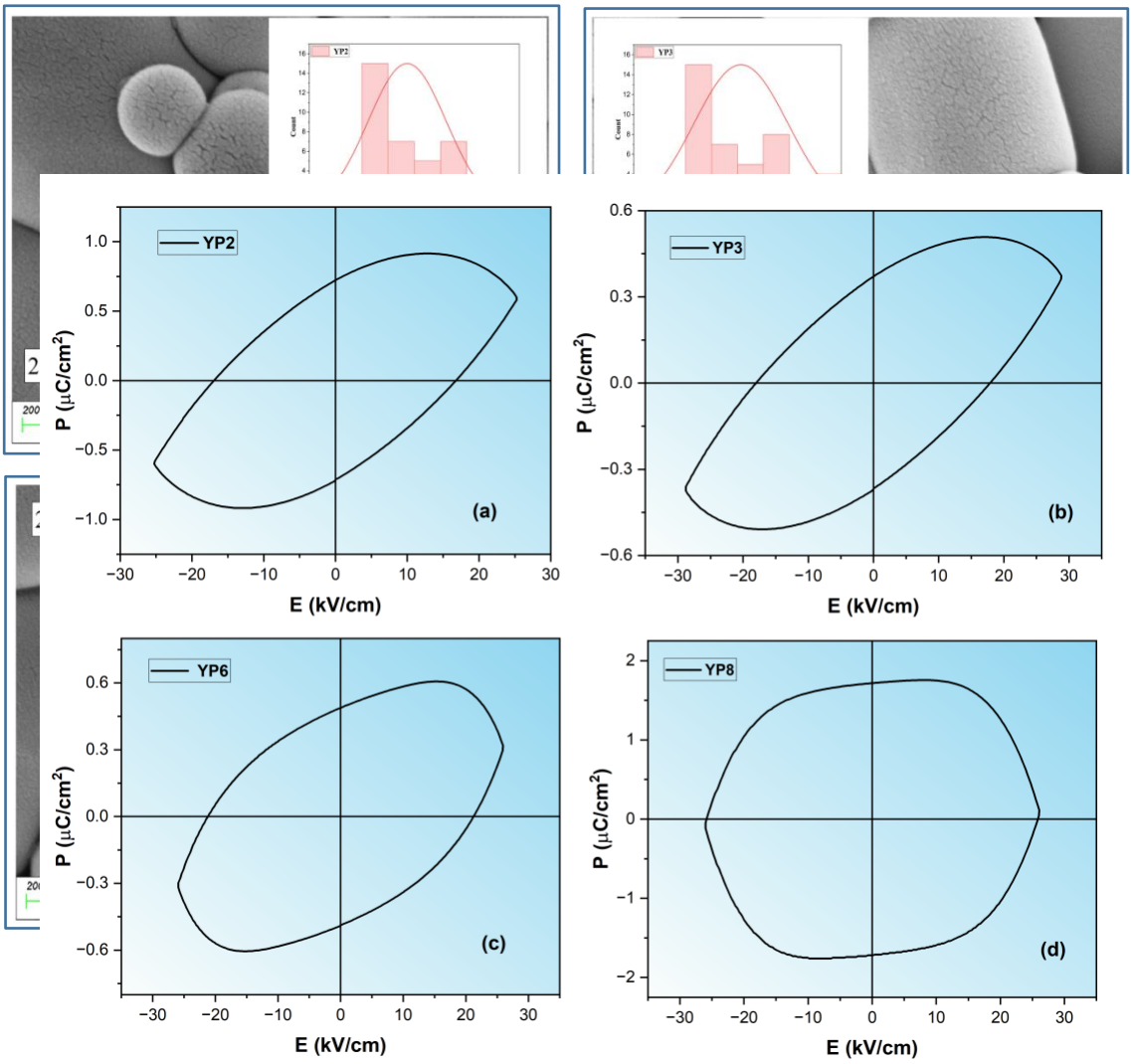

inset Fig 2). Moreover, the two different grains with different shapes seen in YP2 is ascribed to the present of two lattices namely PT and YIG. From the SEM pictures it is evident that with increasing the YIG, the small grains were found to coalesced into single grain. This clearly indicates the complete formation of YIG-PT composites.

Figure 2(a-d). SEM micro graphs of YIG-PT (YP2, YP3, YP6 and YP8) composites.

Fig 3(a-d) illustrates the P-E hysteresis behaviour of YIG - PT composites recorded at room temperature. The graph clearly shows that composites with higher magnetic content (YP8) exhibit broader, more lossy hysteresis loop. This suggests that the presence of a larger proportion of magnetic YIG, which leads to the greater energy dissipation. A possible explanation for this could be the charge separation occurring within the composite lattice. In composites with higher magnetic phase concentrations, the magnetic regions likely to dominate within the local order and influences the ferroelectric (PT) phase. The interaction between the magnetic and ferroelectric/dielectric phases could result in an increased resistance to the reversal of polarization, contributing to the observed loss in energy. The same can be corroborated to tending saturated nature and shape of the hysteresis loop with higher remanet polarisation (Pr) value, as observed in 20YIG-80PT(YP2) composite. But this loop is not exactly ferroelectric nature, instead a lossy nature or dielectric nature. More aspect of this can corroborated to magneto-dielectric studies, which would be discussed in due course.

Figure 3(a-d). P-E loops of YIG-PT composites

The variation of maximum value of polarization with increasing the PT content is shown in the Fig 4. From the plot it is evident that the maximum polarization is found to decrees with increasing the YIG composition and showed higher value for YP8 sample. Moreover, the hysteresis loop shows a circular kind and this nature is being attributed to magnetodielectric nature of the sample.

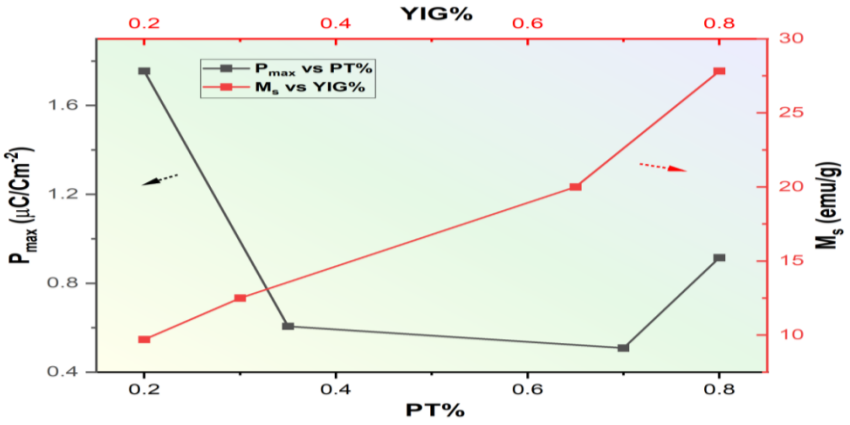

Figure 4. P_{max} vs ($PbTiO_3$) PT% and M_s vs YIG% of YIG-PT composites

Fig 5(a) shows the room temperature Raman spectra of the YIG-PT composite of different weight percentages. The spectra clearly display vibrational modes associated with both the tetragonal PT and the YIG phases. Compared to the pure PT spectrum, noticeable differences are seen in the composite spectra. In particular, the E(1TO), A(1TO), and E(2TO) Raman modes, which are characteristic of the tetragonal PT phase. These phases are distinctly visible and well matches with the results observed in previous studies [21, 22]. Additionally, the plot highlights the presence of the B_1+E mode from the PT phase, along with the Eg mode of the YIG phase. The T_{2g} and E_g modes associated with the YIG phase are also clearly seen in the Raman spectrum.

Fig 5(b) depicts the deconvolution of the Raman modes for the 20YIG-80PT composite, which clearly shows the Raman peaks corresponding to both the PT and YIG phases. This plot indicates that both phases coexist in the composite, with each phase contributing its own unique vibrational modes. The coupling of these modes suggests an interaction between the phases, demonstrating how phase interaction influences the vibrational properties of the composite. Inset Figure 5a clearly shows the how the shoulder peak of YIG-PT composite (YP2) converts to peak of the ferroelectric phase (PT) (marked as dotted region in the Fig 5a). Further, it shows the presence of both the B_1+E and E_g modes.

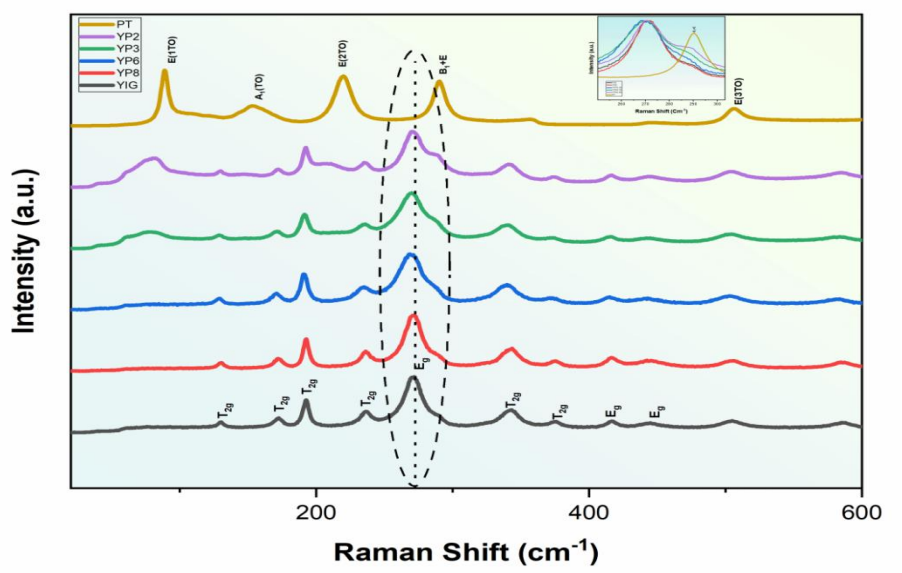

Figure 5(a) Raman analysis of YIG-PT composites

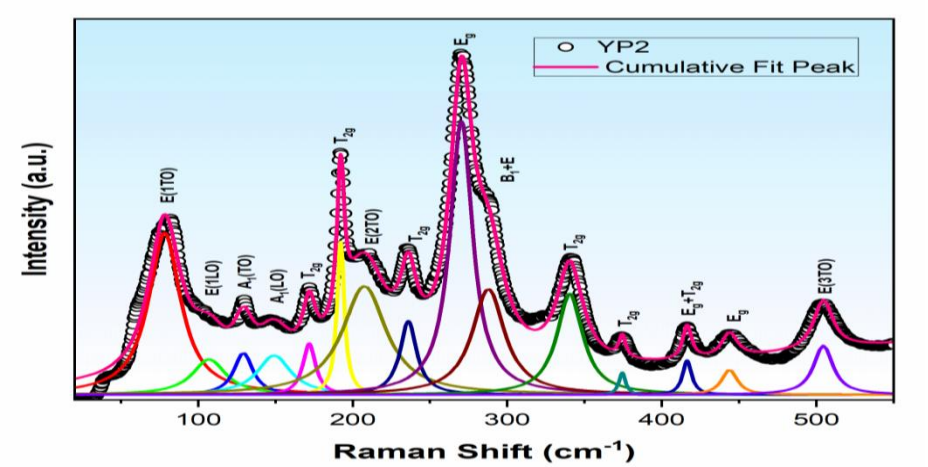

Figure 5(b) Deconvolution of Raman modes of (YP2) 20YIG-80PT composites

Fig 6 shows the M vs H hysteresis behaviour of all the composite samples recorded at room temperature. It is obvious from the plot that the YIG-PT composites exhibit soft magnetic nature as it shows narrow hysteresis loop. It also it shows that the saturation magnetization increases with the increasing of YIG concentration in the composite lattices. The values of saturation magnetization (Ms), Remanent magnetization (Mr), coercive field (Hc) and squareness ratio of the four composites (YP2, YP3, YP6 and YP8) are as given in the Table 2. The squareness factor is a key parameter, which generally ranges from 0 to 1. Composites with (Mr/Ms) ratio lie below 0.5 are typically characterized as multi-domain structures, while those with ratios exceeding 0.5 are considered to exhibit a single-domain magnetic configuration. The squareness ratio (SR) is calculated from the following relation:

$$\text{Squareness Ratio (SR)} = \frac{M_r}{M_s} \qquad (1)$$

Where, M_r is the remanent magnetization, which is the magnetization remaining in the material after the external magnetic field is removed. M_s is the saturation magnetization, which is the maximum magnetization the material can achieve when subjected to a sufficiently large external magnetic field.

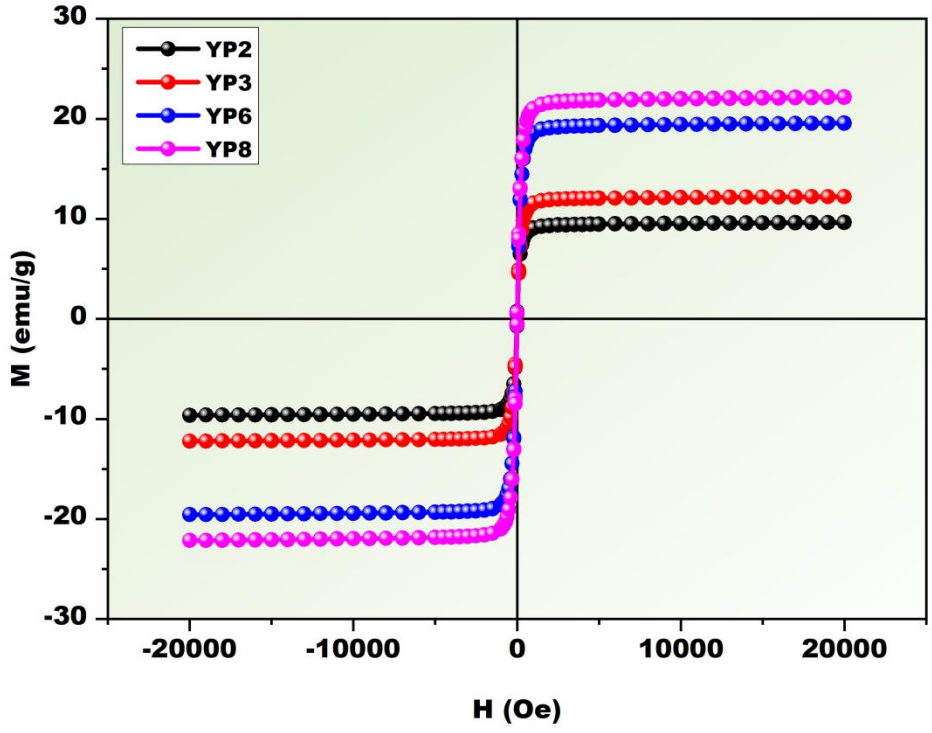

Figure 6. M-H loops of YIG-PT composites

SNo.	Sample Name	Ms (emu/g)	Mr (emu/g)	Hc (Oe)	Mr / Ms
1	20YIG-80PT	9.705	0.719	13.189	0.074
2	30YIG-70PT	12.500	O.477	9.459	0.038
3	65YIG-35PT	19.999	0.550	6.980	0.027
4	80YIG-20PT	27.820	0.638	7.241	0.022

Table 2. Magnetic analysis of the YIG-PT composites

In this study, the squareness values, given in Table 2, were found to range between 0.022 and 0.074, indicating the presence of multiple magnetic domains in the composites. This suggests that the composites are in a multi-domain state rather than a single-domain one.
Fig 4 also depicts the relationship between saturation magnetization and the proportion of Lead Titanate in the YIG-PT composites. The graph clearly demonstrates that an increase in the concentration of YIG within the composite results in a corresponding rise in the saturation magnetization (Ms). This trend can be primarily attributed to the dominance of the ferromagnetic YIG phase over the ferroelectric PT-phase. As YIG is incorporated, the magnetic interactions within the composite are strengthened and finally enhances the overall magnetic response. This suggests that the ferromagnetic properties of YIG play a significant role in shaping the composite's magnetic characteristics, with the ferroelectric phase. To extract more information, the magnetization data is fitted with Law of Approach to Saturation (LAS).

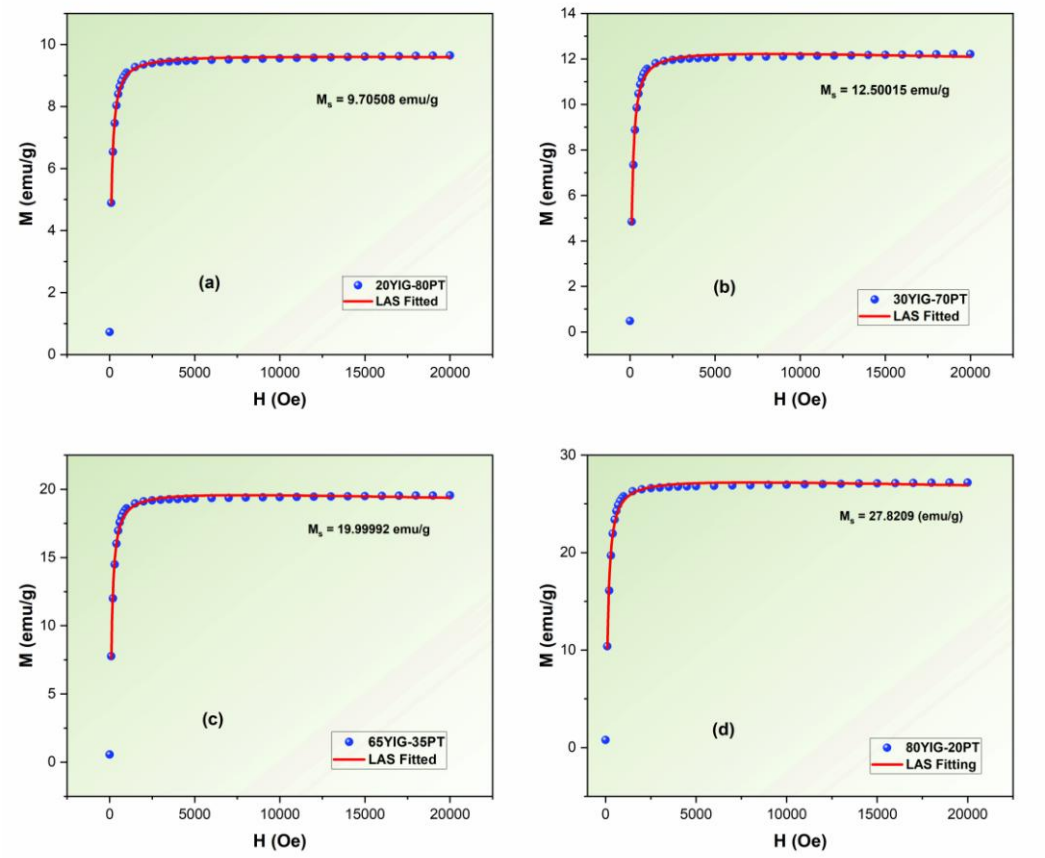

Figure 7(a-d). LAS fittings of YIG-PT composites

Fig 7 (a-d) illustrates the LAS fittings of the YIG-PT composites. These fittings were performed using the Origin software, which allowed for the application of a user-defined function in conjunction with the Levenberg-Marquardt Iteration Algorithm. This iterative algorithm is commonly used to solve nonlinear curve fitting problems, enable us to describe the composite's magnetization behaviours as it approaches

saturation. The Law of Approach to Saturation, which models the relationship between magnetization and applied magnetic field, can be expressed by the following equation:

$$M = M_s\left[1-\frac{a}{H}-\frac{b}{H^2}\right] \quad (2)$$

Here, the term $\frac{a}{H}$ represents magnetic hardness, which explains the structural defects of the sample. The term $\frac{b}{H^2}$ explains the magnetic crystalline anisotropic behaviour of the sample. It is a known that the M_s and M_r are related to the lattice rearrangement bond-angle and cationic bond distances. As mentioned earlier, the complex structure of YIG consists of three different cationic positions, nearly octahedral (24d - site), tetrahedral (16a-site) and dodecahedral site (24c-site), Neel has proposed in his theory that the total magnetic moment of YIG is originated from the magnetic interaction through cation-oxygen anion super exchange interaction between Fe^{3+} ions (Fe^{3+}-O-Fe^{3+}) and Y^{3+} ions. From this one can speculate that the strong coupling of magnetic - piezoelectric/ferroelectric properties may lead to advancements in memory storage devices, which enables us in the development of faster and more efficient storage-conversion devices.

CONCLUSION

The YIG-PT composites were synthesized using the traditional solid-state sintering method, with the sintering process occurring at 1000°C. X-ray diffraction (XRD) patterns of the composites confirm the presence of both YIG and PT phases, indicating their coexistence in the material. The polarization-electric (PE) loops reveal an increase in the energy loss characteristics of the composites as the weight percentage of YIG is increased. Magnetic hysteresis (M vs H) loops demonstrate the soft magnetic behaviour of the composites, with the saturation magnetization rising as the proportion of YIG increases. Additionally, the low squareness ratios observed in all composites, with values below 0.5, suggest the formation of multi domain structures.

The combination of high concentration of YIG and low concentration of PT (80YIG-20PT) composite materials holds great promise for a variety of applications, particularly in the field of magnetoelectric devices that require both magnetic and electric field responses. These multi-dielectric composites could be utilized in applications such as magnetoelectric sensors, multifunctional actuators, and energy harvesting systems.

Acknowledgments: This work is partially supported by AR&DB Project No 2004.

REFERENCES

[1] Verma, S., Maity, M., Maurya, A., et al., 2024, "Evolution of Microstructure, Magnetic and Microwave Properties of Sputter Deposited Polycrystalline YIG Thin Films," J. Mater. Sci.: Mater. Electron., **35**, p. 105.

[2] Khutieva, A. B., Sadovnikov, A. V., Garanin, F. E., Anisimov, R. A., Kalinova, A. E., Chen, X., Song, Y., Sheshukova, S. E., and Lomova, M. V., 2025, "Spin Wave Propagation in YIG Waveguides With Magnetic Microvolcanoes: Experiment and Simulation," Appl. Phys. Lett., **126**(6), p. 062402.

[3] Da, B. F. E., Dufay, B., and Saez, S., 2025, "Four-Port Characterization of YIG Magnonic Device: A Way to Improve Magnetic Sensors Based on YIG Device," IEEE Trans. Magn.

[4] Zenbaa, N., et al., 2025, "YIG/CoFeB Bilayer Magnonic Isolator," IEEE Magn. Lett.

[5] Pradhan, D. K., Kumari, S., and Rack, P. D., 2020, "Magnetoelectric Composites: Applications, Coupling Mechanisms, and Future Directions," Nanomaterials, **10**(10), p. 2072.

[6] Mao, Q., Wu, J., Hu, Z., Xu, Y., Du, Y., Hao, Y., Guan, M., Wang, C., Wang, Z., Zhou, Z., Dong, S., Ren, W., Liu, M., and Jiang, Z., 2021, "Magnetoelectric Devices Based on Magnetoelectric Bulk Composites," J. Mater. Chem. C, **9**, pp. 5594–5614.

[7] Wen, D., Zhang, J., Kulikov, A., Cui, J., Chen, Z., Wang, Z., Zhang, Q., Guo, J., and Li, R., 2025, "The Effect of Al^{3+} Ion Substitution on Microwave Dielectric and Magnetic Properties of YIG Ferrites," Ceram. Int., **51**(5), pp. 6272–6280.

[8] Xu, J., Horn, C., Jiang, Y., Pishehvar, A., Li, X., Rosenmann, D., Han, X., Levy, M., Guha, S., and Zhang, X., 2025, "Cryogenic Hybrid Magnonic Circuits Based on Spalled YIG Thin Films," J. Appl. Phys., **137**(2), p. 023901.

[9] Tiwari, S., Ashok, A., Devitt, C., et al., 2025, "High-Performance Magnetostatic Wave Resonators Based on Deep Anisotropic Etching of Gadolinium Gallium Garnet Substrates," Nat. Electron.

[10] Lisnevskaya, I. V., and Aleksandrova, I. A., 2020, "Magnetoelectric Composites of Lead-Free Piezoelectrics and Yttrium Iron Garnet: Interfacial Reactions and Functional Properties," Appl. Phys. A, **126**, p. 406.

[11] Yang, H., Zhang, G., Lin, Y., Ye, T., and Kang, P., 2015, "Electrical, Magnetic and Magnetoelectric Properties of $BaTiO_3/BiY_2Fe_5O_{12}$ Particulate Composites," Ceram. Int., **41**(5), pp. 7227–7232.

[12] Schileo, G., Pascual-Gonzalez, C., Alguero, M., Reaney, I. M., Postolache, P., Mitoseriu, L., Reichmann, K., and Feteira, A., 2016, "Yttrium Iron Garnet/Barium Titanate Multiferroic Composites," J. Am. Ceram. Soc., **99**, pp. 1609–1614.

[13] Akyol, M., Aka, C., İnözü, O., et al., 2023, "Absorbing the Entire X-Band via Conductive Polymer Polyaniline Coated $Y_3Fe_5O_{12}/NiFe_2O_4$ Hybrid Composites," J. Mater. Sci.: Mater. Electron., **34**, p. 544.

[14] Lin, Y., Liu, X., Ye, T., et al., 2016, "Synthesis and Characterization of $CoFe_2O_4/Y_3Fe_5O_{12}$ Composites Based on Polyaniline," J. Mater. Sci.: Mater. Electron., **27**, pp. 4833–4838.
[15] Lisnevskaya, I. V., Bobrova, I. A., Lupeiko, T. G., Agamirzoeva, M. R., and Myagkaya, K. V., 2016, "$Y_3Fe_5O_{12}$/Na,Bi,Sr-Doped PZT Particulate Magnetoelectric Composites," J. Magn. Magn. Mater., **405**, pp. 62–65.
[16] Haertling, G. H., 1999, "Ferroelectric Ceramics: History and Technology," J. Am. Ceram. Soc., **82**(4), pp. 797–818.
[17] Jian, G., Jiao, Y., Meng, Q., Guo, Y., Wang, F., Zhang, J., Wang, C., Moon, K.-S., and Wong, C.-P., 2021, "Excellent High-Temperature Piezoelectric Energy Harvesting Properties in Flexible Polyimide/3D $PbTiO_3$ Flower Composites," Nano Energy, **82**, p. 105778.
[18] Susneha, T., Someshwar, P., and Prasad, N. V., 2024, "Electrical, Magnetic, and Raman Spectroscopic Studies on Bi-Modified YIG Ceramics," J. Mater. Sci.: Mater. Electron., **35**, p. 968.
[19] Chen, T.-Y., Chu, S.-Y., Chang, R.-C., Cheng, C.-K., Hong, C.-S., and Nien, H.-H., 2007, "The Characteristics of Low-Temperature Sintered $PbTiO_3$ Based Ceramics and Its Applications," Sens. Actuators A Phys., **134**, pp. 452–456.
[20] Thirumalasetty, Avanish Babu., Krishnan, T., Kota Venkata, S. K., Adiraj, S., Xavier, D., Venkatachalam, S., Reddy, R. G. K., Dudekula, Z., and Wuppulluri, M., 2023, "(Title Missing)," ACS Appl. Electron. Mater., **5**(6), pp. 3120–3129.
[21] Frantti, J., and Lantto, V., 1996, "Raman Studies Between 11 and 300 K of the Effects of Nd Additive in Ferroelectric Lead-Titanate Ceramics," Phys. Rev. B, **54**, p. 12139.
[22] Pinto, A. H., Souza, F. L., Longo, E., Leite, E. R., and Camargo, E. R., 2011, "Structural and Dielectric Characterization of Praseodymium-Modified Lead Titanate Ceramics Synthesized by the OPM Route," Mater. Chem. Phys., **130**(1–2), pp. 259–263.